

Green Chemistry

Cutting-edge research for a greener sustainable future

Accepted Manuscript

View Article Online
View Journal

This article can be cited before page numbers have been issued, to do this please use: N. R. Nicomel, L. Otero-Gonzalez, L. Arashiro, M. Garfi, I. Ferrer, P. Van Der Voort, K. Verbeken, T. Hennebel and G. Du Laing, *Green Chem.*, 2020, DOI: 10.1039/C9GC03073E.



This is an Accepted Manuscript, which has been through the Royal Society of Chemistry peer review process and has been accepted for publication.

Accepted Manuscripts are published online shortly after acceptance, before technical editing, formatting and proof reading. Using this free service, authors can make their results available to the community, in citable form, before we publish the edited article. We will replace this Accepted Manuscript with the edited and formatted Advance Article as soon as it is available.

You can find more information about Accepted Manuscripts in the [Information for Authors](#).

Please note that technical editing may introduce minor changes to the text and/or graphics, which may alter content. The journal's standard [Terms & Conditions](#) and the [Ethical guidelines](#) still apply. In no event shall the Royal Society of Chemistry be held responsible for any errors or omissions in this Accepted Manuscript or any consequences arising from the use of any information it contains.

1 **Microalgae: A sustainable adsorbent with high potential for upconcentration**
2 **of indium(III) from liquid process and waste streams**

3

Nina Ricci Nicomel^{a,*}, Lila Otero-Gonzalez^a, Larissa Arashiro^{a,b}, Marianna Garfi^b, Ivet Ferrer^b, Pascal Van Der Voort^c, Kim Verbeken^d, Tom Hennebel^e, Gijs Du Laing^a

4

5 ^a Laboratory of Analytical Chemistry and Applied Ecochemistry, Department of Green
6 Chemistry and Technology, Ghent University, Coupure Links 653, 9000 Ghent, Belgium

7 ^b Group of Environmental Engineering and Microbiology, Department of Civil and
8 Environmental Engineering, Universitat Politècnica de Catalunya·BarcelonaTech, c/ Jordi
9 Girona 1-3, Building D1, 08034 Barcelona, Spain

10 ^c Center for Ordered Materials, Organometallics and Catalysis, Department of Inorganic and
11 Physical Chemistry, Ghent University, Krijgslaan 281 (S3), 9000 Ghent, Belgium

12 ^d Department of Materials, Textiles and Chemical Engineering, Ghent University,
13 Technologiepark Zwijnaarde 46, 9052 Zwijnaarde, Belgium

14 ^e Center for Microbial Ecology and Technology, Department of Biochemical and Microbial
15 Technology, Ghent University, Coupure Links 653, 9000 Ghent, Belgium

16

17

18 * Corresponding author:

19 E-mail: NinaRicci.Nicomel@UGent.be

20 Tel.: +3292646131

21 Fax: +3292646232

22

23 **ABSTRACT**View Article Online
DOI: 10.1039/C9GC03073E

24 Indium (In) is a critical raw material heavily demanded in the optical-electronics industry. With
25 its high supply risk, sustainable technologies are needed to recover In(III) from secondary
26 sources, such as leachates from sludge produced by zinc processing industries (e.g., jarosite)
27 and indium tin oxide etching wastewater. This study presents In(III) biosorption as an eco-
28 friendly alternative to conventional physicochemical recovery technologies. The characteristics
29 of In(III) adsorption by microalgal biomass were investigated in batch experiments. Adsorption
30 isotherm was well-fitted by the Freundlich model. The estimated maximum adsorption capacity
31 of In(III) was 0.14 mmol/g of microalgae, which is higher than that of some chemically
32 modified adsorbents reported in the literature. Selectivity of In(III) was also observed over other
33 metals, such as Cu(II), Zn(II), and Al(III). Furthermore, the microalgae biosorbent was
34 regenerated using a 0.1 M HCl solution, with up to 80% In(III) recovery, for several cycles.
35 From these results, microalgae prove to have potential for In(III) biosorption from aqueous
36 solutions.

37
38 **Keywords:** Indium, microalgae, biosorption, desorption, wastewater
39

40 1. Introduction

41 Indium (In) is a relatively rare metal present in minor amounts in the Earth's crust at
42 approximately 0.05 ppm and 0.072 ppm for the continental and oceanic crusts, respectively
43 (Schwarz-Schampera and Herzig, 2002). Because of these low concentrations, the mining of
44 In(III) as primary commodity is uneconomic (Schwarz-Schampera, 2014). Nonetheless, traces
45 of In(III) occur in some minerals such as sphalerite (ZnS), chalcopyrite (CuFeS₂), cassiterite
46 (SnO₂), and galena (PbS) (Felix, 2000), which enables In(III) extraction from the by-products
47 formed during zinc, copper, and tin production (Alfantazi and Moskalyk, 2003).

48 In(III) is extensively used in electronic and energy-related industries, particularly in the
49 production of indium tin oxide (ITO) thin-film coatings for flat-panel displays and solar cells
50 (Hasegawa et al., 2013; USGS, 2018). Due to this increasing demand and limited supply of
51 primary resources, the European Commission has listed In(III) as one of the 27 raw materials
52 critical for the European Union (EU) (European Commission, 2017). Two particular concerns
53 for In(III) criticality are the geopolitical challenges associated with the concentration of reserves
54 and production in particular countries and the low substitution and recycling rates. For example,
55 In(III) from waste liquid crystal display (LCD) panels is barely recycled (European
56 Commission, 2017; Sun et al., 2017). For these reasons, there has been a growing interest in the
57 recovery of In(III) from secondary sources, such as leachates from polymetallic sludge
58 produced during zinc refining and waste solutions from ITO etching processes (Chou et al.,
59 2016; Orko et al., 2016). For instance, jarosite (MFe₃(SO₄)₂(OH)₆, where M is a metal cation
60 (e.g., Na, K, Pb) or ammonium) is a solid industrial byproduct produced from the iron removal
61 in the hydrometallurgical zinc winning process (Wegscheider et al., 2017, Orko et al., 2016).
62 This sludge contains some critical raw materials, including In(III) and Ag(I). In a pre-feasibility
63 study of processing jarosite sludge to value-added products performed by Orko et al. (2016),
64 the In(III) content in jarosite was approximately 0.9 mol/t, which is equivalent to 0.36

65 megamoles In/yr for a plant processing 400,000 t/yr of jarosite. Being an abundant source of
66 In(III) and other critical metals, interest in jarosite leaching has been increasing during the last
67 few years, especially taking into account that worldwide jarosite production ranges from 5 to 6
68 Mt per year (Wilson et al., 2016). Depending on the leaching agent and operational parameters
69 used in leaching the jarosite sludge, the concentration of In(III) in the leachate normally ranges
70 from 0.5 to 2.2 mM (Koleini et al., 2010; Zhang et al., 2016).

71 Many technologies have been proposed for In(III) recovery from liquid process and waste
72 streams, with solvent extraction and commercial ion exchange resins being two of the most
73 widely used (Yang et al., 2013; Chou et al., 2016; Fortes et al., 2003). However, these
74 conventional methods present disadvantages, such as high reagent and energy requirements,
75 high capital and operational costs, and generation of toxic sludge or other waste products (Ogi
76 et al., 2012). Furthermore, when In(III) concentration of the stream is low, these technologies
77 are unfavorable because of the resulting low recovery (Hasegawa et al., 2013). For instance,
78 applying solvent extraction to dilute streams would require an aqueous/organic solvent ratio of
79 about 1 to provide satisfactory phase separation (Tarkan and Finch, 2005). However,
80 maintaining this ratio would not result to concentration enrichment. In many cases, waste
81 streams have dilute In(III) concentrations, such as those obtained from leaching end-of-life
82 LCD panels (Rocchetti et al., 2015). Thus, it is important to develop more economical,
83 effective, and environment-friendly methods to recover In(III).

84 Biosorption can be an alternative technology considering that a number of biosorbents can
85 effectively bind and concentrate metals even from very dilute solutions (Ogi et al., 2012). This
86 technique has not been much explored for In(III) recovery, although it presents a great potential
87 and an eco-friendly alternative to conventional physicochemical technologies. Among widely
88 available biosorbents, microalgal biomass possesses relatively high binding capacities for
89 several metals (Wilde and Benemann, 1993; Aksu, 2002). This can be explained by the presence

90 of carboxylic, hydroxyl, amino, phosphate, and sulfhydryl groups in the microalgal cell wall
91 that can act as metal binding sites (Suresh Kumar et al., 2015). To date, the potential of using
92 microalgal biomass to remove and/or recover In(III) from aqueous solutions has not been
93 investigated.

94 In the present work, the use of microalgal biomass was studied for the removal and recovery
95 of In(III) from aqueous solutions. Different process parameters—pH, contact time, initial
96 indium concentration and presence of competing ions—were studied to assess their effects on
97 In(III) biosorption. In addition, the desorption of indium ions adsorbed on the microalgal
98 biomass was investigated with various desorbing agents.

99 2. Materials and methods

100 2.1 Chemicals

101 All chemicals were of analytical grade. Single-metal stock solutions (20 mM) were prepared
102 by dissolving InCl₃, AlCl₃, CuCl₂·2H₂O, SnCl₂·2H₂O, ZnCl₂, and FeCl₃·6H₂O in ultrapure
103 water (resistivity > 18.2 MΩ·cm). Solutions of 1 M HCl and 0.1 M NaOH were used to adjust
104 the pH. The laboratory glassware was washed with 5% HNO₃ and rinsed with ultrapure water
105 before use.

106 2.2 Cultivation and preparation of the microalgae biosorbent

107 Microalgae were cultivated in an outdoor pilot plant at the laboratory of the GEMMA
108 Research Group (Universitat Politècnica de Catalunya, Barcelona, Spain). The system treated
109 real municipal wastewater that received a screening pre-treatment before being pumped into a
110 homogenization tank. The wastewater was pumped from this tank into a primary settler
111 followed by a high rate algal pond (HRAP) (nominal volume of 0.5 m³) and a secondary
112 clarifier, where the effluent was separated from the microalgal biomass. The biomass used in
113 this study was harvested during June 2017. The culture was dominated by *Chlorella* sp. and
114 diatoms (mostly *Nitzschia* sp. and *Navicula* sp.), with the presence of grazers (ciliate and

115 flagellate protozoans). More details regarding the operational parameters and microbiological
116 characteristics can be found in a previous study (Arashiro et al., 2019). Harvested biomass was
117 thickened in laboratory Imhoff cones stored at 4°C for 24 hours. Thickened microalgal biomass
118 was then centrifuged at 4,200 rpm for 10 minutes (Orto Alresa, Spain). The supernatant was
119 discarded and the microalgae paste was frozen at -80°C overnight in an ultra-freezer (Arctiko,
120 Denmark) and finally lyophilized for 24 hours (-110 °C, 0.049 hPa) (Scanvac, Denmark).
121 Because of its high pH, the microalgal biomass was repeatedly washed with ultrapure water
122 and dried in an oven at 50°C for 24 hours. Afterwards, it was ground to a particle size <1 mm.
123 Light microscope images of the microalgal biomass before and after grinding are shown in
124 Figure S1 in the Supplementary Information. These indicate that the preliminary grinding does
125 not affect the cellular structure and cell wall integrity of the microalgae.

126 *2.3 Fourier transform infrared spectroscopy*

127 Fourier transform infrared (FTIR) spectroscopy spectra were used to identify the functional
128 groups on the microalgal biomass surface and to determine which of these functional groups
129 are possibly responsible for In(III) biosorption. FTIR measurements were performed on raw
130 and In-loaded microalgal biomass using a Thermo Scientific Nicolet 6700 FT-IR Spectrometer.
131 The In-loaded microalgal biomass was obtained by performing In(III) biosorption. Afterwards,
132 the phase separation was done through centrifugation, wherein the supernatant was discarded
133 and the pellet was dried at 50°C for 24 h. For both raw and In-loaded biosorbents, a dried and
134 ground sample (ca. 15 mg), mixed with a few milligrams of potassium bromide (KBr), was
135 placed on a disc of KBr powder pressed in a micro-cup. FTIR spectra were recorded within the
136 wavenumber range of 400 to 4000 cm⁻¹ with spectral resolution of 4 cm⁻¹ and 256 scans.
137 Background measurements were performed with pure KBr and automatically subtracted from
138 each sample spectrum. All spectra were plotted using the Thermo Scientific™ OMNIC™
139 Spectra software.

140 2.4 Scanning electron microscopy

141 The effects of adsorption and desorption on the surface morphology of the microalgal
142 biomass were investigated using scanning electron microscopy (SEM). The tests were
143 conducted using raw, In(III)-loaded, and In(III)-desorbed microalgal biomass. Before
144 measurement, the samples were fixed in 3% glutaraldehyde with 0.1 M phosphate buffer for 3
145 hours at room temperature. The samples were then rinsed three times with 0.1 M phosphate
146 buffer for 10 minutes each. Afterwards, the samples were dehydrated for 10 minutes in each of
147 the graded ethanol solutions of increasing concentration (i.e., 30%, 50%, 70%, 80%, 90%, 95%,
148 and 100%). The dehydrated microalgal biomass was dried using the chemical drying agent
149 hexamethyldisilazane (HMDS). The dried samples were mounted on a stub and gold-sputtered
150 prior to measurement. The images of the microalgal biomass were taken with a JEOL JSM-
151 7600F field emission scanning electron microscope.

152 2.5 Acidic and basic surface properties

153 The surface groups of the microalgal biomass causing the acidic and basic surface properties
154 were estimated using Boehm titration (Boehm, 2002). Microalgal biomass (0.45 g) was added
155 to a series of 50-mL centrifuge tubes containing 45 mL of the following solutions each: 0.1 M
156 NaHCO_3 , 0.05 M Na_2CO_3 , 0.1 M NaOH , and 0.1 M HCl . The suspensions were shaken in an
157 orbital shaker at 115 rpm. After 48 hours, these were filtered using membrane syringe filters of
158 0.45- μm pore size. Subsequently, 10 mL of each filtrate was titrated with either 0.1 M HCl or
159 NaOH depending on the starting solution. The concentrations of the surface oxygen groups
160 causing the acidic properties were calculated based on the following assumptions: (1) NaHCO_3
161 deprotonates carboxylic groups only, (2) Na_2CO_3 deprotonates carboxylic groups and reacts
162 with lactones through hydrolytic ring opening, and (3) NaOH deprotonates both carboxylic and
163 phenolic groups, and reacts with lactones through hydrolytic ring opening. Similarly, the
164 amount of basic sites was calculated from the amount of HCl that reacted with the biosorbent.

165 2.6 Effect of pH on indium biosorption

View Article Online
DOI: 10.1039/C9GC03073E

166 The effect of pH on indium biosorption was investigated to determine the optimum pH
167 required for the adsorption kinetic and equilibrium experiments. An indium solution (0.15 mM)
168 was prepared from the In(III) stock solution. Ten milliliters of this solution was transferred into
169 each 12-mL polypropylene centrifuge tube containing 100 mg of microalgal biomass. To avoid
170 precipitation of In(OH)₃, which starts at around pH 2.7 as determined from control experiments
171 (Figure S2 in the Supplementary Information), the initial pH was adjusted to values from 1 to
172 2, considering the increase in the final pH of the solution once this is put in contact with the
173 microalgal biomass. Samples were shaken in an orbital shaker at 115 rpm for 24 hours.
174 Afterwards, the final pH was measured using a Thermo Scientific Orion Star A211 pH meter.
175 The phase separation was done through filtration using membrane filters of 0.45 μm pore size.
176 Indium concentrations in the filtrate were measured using inductively coupled plasma mass
177 spectrometry (ICP-MS, Perkin Elmer NexION 350). All experiments were conducted in
178 duplicate and data are presented as mean values with standard deviation.

179 The removal efficiency and adsorption capacity of the microalgal biomass were calculated
180 using equations 1 and 2, respectively.

$$181 \text{ Removal efficiency (\%)} = \frac{C_0 - C_e}{C_0} \times 100 \quad (1)$$

$$182 q = \frac{(C_0 - C_e) \times V}{m} \quad (2)$$

183 Where q is the amount of In(III) adsorbed per unit mass of microalgal biomass (mmol/g), C_0 is
184 the initial In(III) concentration (mM), C_e is the equilibrium In(III) concentration (mM), V is the
185 volume of In(III) solution (L), and m is the mass of the biosorbent (g).

186 2.7 Biosorption kinetic experiments

187 Batch experiments were performed to study the kinetics of In(III) adsorption on microalgal
188 biomass. Samples were prepared as described in Section 2.6. The initial pH values of the

189 solutions were adjusted to the optimum pH. Immediately after putting the biosorbent in contact
190 with the In(III) solution, the suspensions were shaken for different time intervals ranging from
191 30 minutes to 24 hours. After the predefined intervals, each sample was filtered using a syringe-
192 type membrane filter of 0.45 μm pore size to separate the biosorbent from the liquid phase. The
193 In(III) concentrations of the filtrate were then determined by ICP-MS.

194 *2.8 Biosorption equilibrium experiments*

195 The adsorption of In(III) on microalgal biomass was assessed at different concentrations in
196 order to study the effect of concentration on the amount of In(III) adsorbed and to determine
197 the maximum adsorption capacity of the microalgal biomass. Batch biosorption experiments
198 were performed using the same procedure described in Section 2.6, except that the optimum
199 pH was used and that the initial In(III) concentration was varied from 0.05 to 10 mM. After
200 reaching equilibrium, the final pH values of the samples were measured, followed by phase
201 separation. The In(III) concentrations of the filtrate were measured using ICP-MS. The obtained
202 results were fitted to Langmuir and Freundlich adsorption models, which are presented by
203 equations 3 and 4, respectively. The adsorption isotherms and the corresponding parameters
204 were determined using SigmaPlot Version 13.0.

$$205 \quad q_e = \frac{q_{\max} b C_e}{1 + b C_e} \quad (3)$$

$$206 \quad q_e = K_f C_e^{1/n} \quad (4)$$

207 Where q_e is the amount of In(III) adsorbed per unit mass of microalgal biomass at equilibrium
208 (mmol/g), q_{\max} is the maximum adsorption capacity (mmol/g), b is the Langmuir adsorption
209 equilibrium constant (L/mmol), C_e is the equilibrium In(III) concentration (mM), K_f is the
210 Freundlich constant ($\text{mmol}^{1-1/n} \text{L}^{1/n}/\text{g}$) and $1/n$ is a dimensionless parameter that varies between
211 0 and 1.

212 *2.9 Effect of competing ions on indium biosorption*

213 The competing ions studied in this work were Cu(II), Zn(II), Sn(II), Al(III), and Fe(III).
214 Stock solutions were prepared by combining In(III) and the ion of interest. In order to allow
215 competition for adsorption sites, the concentration of the competing ions should be high enough
216 to saturate the microalgal biomass. By determining the maximum adsorption capacity of the
217 microalgal biomass for each of the competing ions at an initial pH of 2 (Table S1 in the
218 Supplementary Information), a concentration of 10 mM was chosen for the competing ions.
219 The initial In(III) concentration was set to 1 mM and the initial pH of the solution was adjusted
220 to around pH 2. Samples were shaken in an orbital shaker for 24 hours at 115 rpm. This was
221 followed by phase separation through filtration, then by the analysis of In(III) concentrations
222 using ICP-MS.

223 2.10 Desorption experiments

224 Prior to desorption, an In(III) adsorption experiment was first completed. This was carried
225 out at pH 2 with an initial In(III) concentration of 0.15 mM. Specifically for this adsorption
226 experiment, phase separation was carried out through centrifugation at 10,000 rpm for 10
227 minutes using an Eppendorf Centrifuge 5804 R. The amount of In(III) adsorbed by the
228 microalgal biomass (m_{ads}) was calculated from the initial and final In(III) concentrations in the
229 solution using equation 5.

$$230 \quad m_{ads} = (C_0 - C_e)V \quad (5)$$

231 Where C_0 is the initial In(III) concentration (mM), C_e is the equilibrium In(III) concentration
232 (mM), and V is the volume of In(III) solution (L).

233 For the desorption experiments, the supernatant was removed from the centrifuge tubes.
234 This was followed by the addition of 10 mL of 0.1 M desorbing agent to the previously In-
235 loaded microalgal biomass. Tested desorbing agents include HCl, HNO₃, NaCl, CaCl₂, and
236 ethylenediaminetetraacetic acid (EDTA). The suspensions were shaken at 115 rpm using an
237 orbital shaker at room temperature for 24 hours. The In(III) desorption efficiencies were

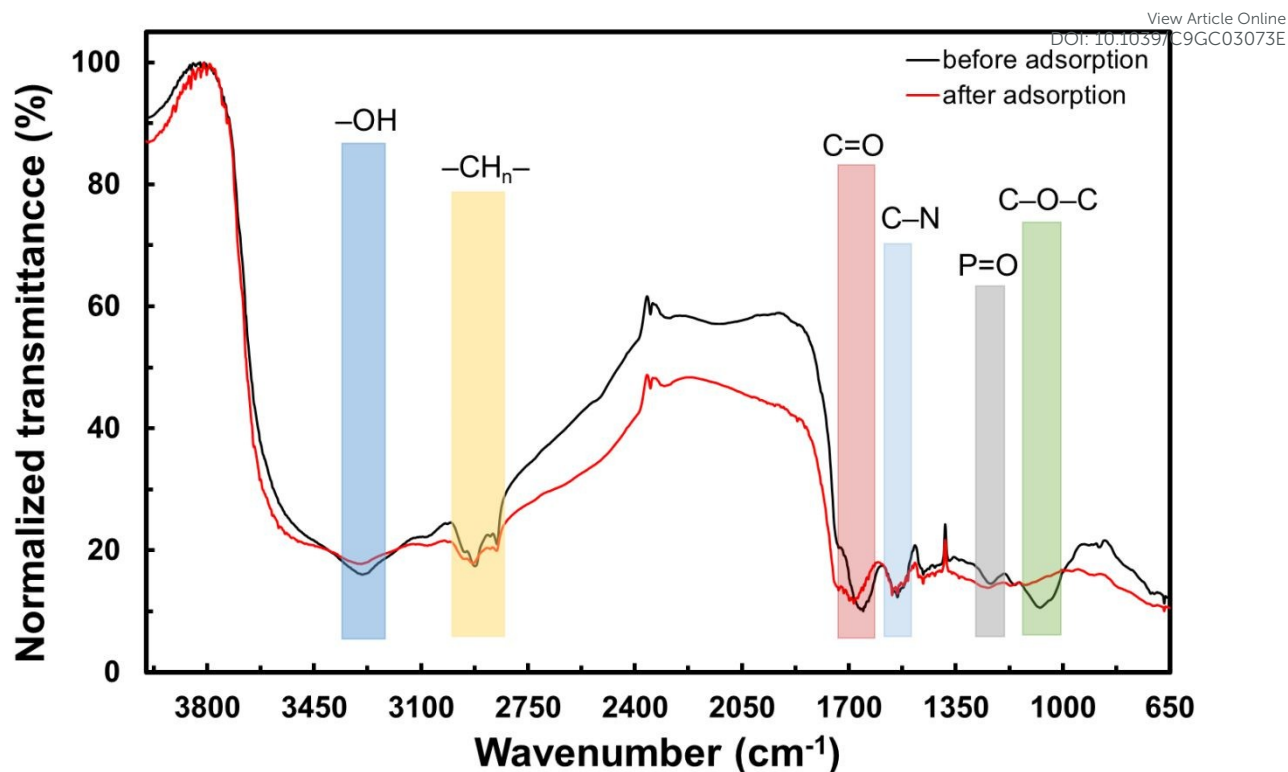
238 calculated as the ratio of the amount of In(III) desorbed to the amount of In(III) adsorbed. After
239 choosing the most favorable desorbing agent, the optimal desorption conditions (i.e., liquid-to-
240 solid (L/S) ratio and desorption time) were determined.

241 For the regeneration experiments, five adsorption-desorption cycles were performed in the
242 most effective desorption conditions. After each desorption step, the microalgal biomass was
243 washed three times with Milli-Q water to remove traces of the desorbing agent. The biosorbent
244 was dried afterwards at 50°C for 24 hours, and weighed to obtain the mass lost after the
245 desorption step.

246 3. Results and Discussion

247 3.1 FTIR analysis

248 The FTIR spectra of the microalgal biomass (Figure 1) showed different characteristic peaks
249 implying that a variety of functional groups may be present on the biosorbent's surface. These
250 peaks were observed at around 3275 cm⁻¹, 3000-2840 cm⁻¹, 1600 cm⁻¹, 1525 cm⁻¹, 1200 cm⁻¹,
251 and 1100 cm⁻¹, which are indicative of -OH, -CH_n-, C=O, C-N, P=O, and C-O-C groups,
252 respectively. The shifts in band wavenumber or differences in vibration intensity between the
253 spectra of raw and metal-loaded biosorbents may indicate the functional groups primarily
254 involved in metal biosorption (Dmytryk et al., 2014). For the spectrum of the In-loaded
255 microalgal biomass, marginal differences were observed compared to that of the raw microalgal
256 biomass.



257 **Figure 1.** Normalized FTIR spectra of microalgal biomass before (black) and after (red) In(III)
 258 biosorption.

259 3.2 Scanning electron microscopy

260 The surface morphological characteristics of the microalgal biomass before and after In(III)
 261 biosorption were compared through SEM images. The image of the microalgal biomass before
 262 biosorption revealed that the microalgal biomass has an irregular surface and very low porosity
 263 (Figure S3A in the Supplementary Information). The pores have different shapes and sizes,
 264 which are mostly mesoporous. Nitrogen sorption measurements confirmed the low porosity of
 265 this biosorbent with a pore volume of 0.000303 cm³/g. Figure S3B in the Supplementary
 266 Information shows a SEM image of the microalgal biomass after biosorption. In general, there
 267 is no significant difference between the surfaces of the microalgal biomass before and after
 268 In(III) biosorption. It can also be seen in Figure S4 that the structure of the particles did not
 269 change before and after the biosorption process.

270 3.3 Surface groups of the microalgal biomass causing acidic and basic surface properties

271 Boehm titration was used to characterize the surface chemistry of the microalgal biomass. View Article Online
DOI: 10.1039/C9GC03073E

272 This method has the advantages of being simple, fast, and usually reproducible. However, one

273 disadvantage of this method is that all groups are classified as oxygen-containing acids. All

274 other groups, which contain nitrogen, phosphorus, or sulfur for instance, will be considered as

275 carboxylic acids, lactones, or phenols because the selectivity is based on the pK_a values of the

276 surface species (Bandosz et al., 2003). Table 1 shows the amounts of carboxylic, lactonic,

277 phenolic, and basic groups that were estimated on the surface of the microalgal biomass. The

278 results indicate that more basic groups (1.79 mmol/g) are present on the biosorbent's surface

279 compared to the other surface groups giving the acidic properties. It was also observed that the

280 carboxylic group is the predominant group causing the surface acidity at 0.36 mmol/g.

281 Carboxylic groups are widely reported as the main functional group involved in metal binding

282 in microalgae (Dmytryk et al., 2014; Monteiro et al., 2012; Suresh Kumar et al., 2015).

283 **Table 1.** Amount of surface groups giving the acidic and basic properties of the microalgal

284 biomass as determined through Boehm titration.

Surface groups	Amount (mmol/g)
Carboxylic	0.36
Lactonic	0.21
Phenolic	0.23
Basic sites	1.79

285

286 *3.4 Effect of pH on indium biosorption*

287 Solution pH plays an important role in metal biosorption since it influences both the surface

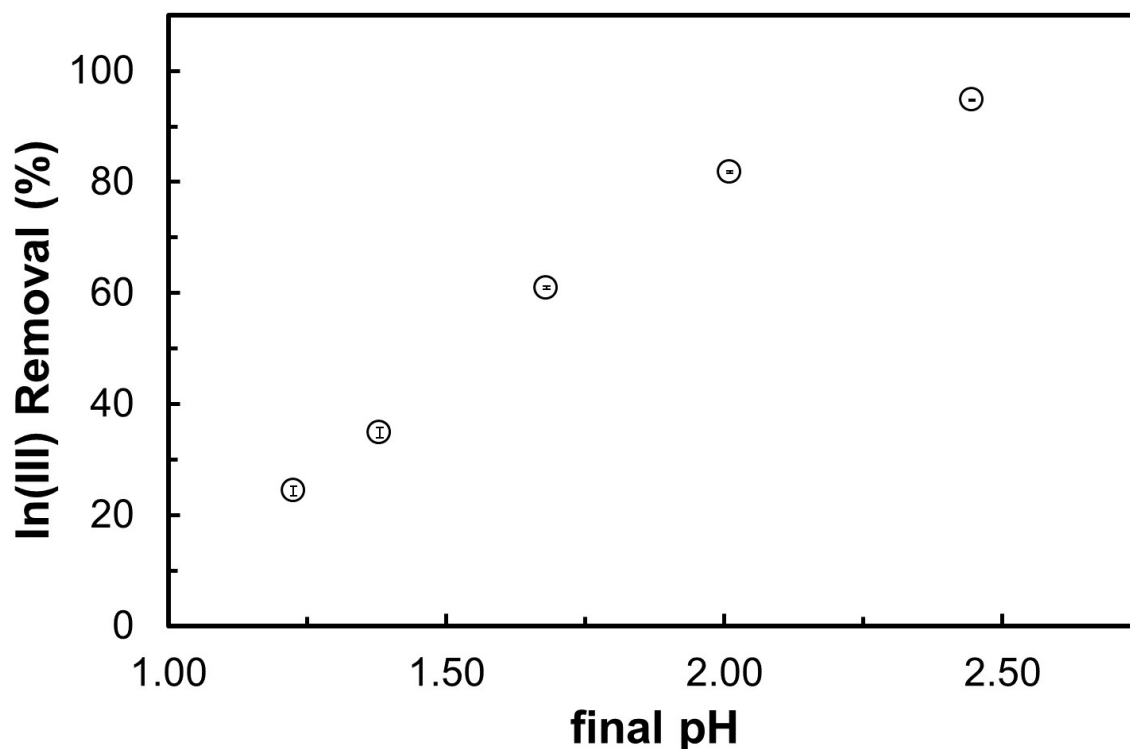
288 charge of the biosorbent and the distribution of metal species in the solution (Suresh Kumar et

289 al., 2015). In(III) removal increased with increasing pH (Figure 2). Particularly, the In(III)

290 adsorption largely increased by 70% as the final pH increased from 1.23 to 2.45. The maximum

291 In(III) adsorption (94.7% of initial In) was obtained at the initial pH of 2, so this pH value was
292 chosen for further biosorption experiments.

293



294 **Figure 2.** Effect of pH on indium removal efficiency. Experimental conditions: initial In(III)
295 concentration = 0.15 mM; L/S ratio = 100 mL/g; contact time = 24 hours; room temperature.

296 In the studied system and pH range, the main chemical species of indium in the solution is
297 In^{3+} . This is based on the speciation diagram of 0.15 mM indium in aqueous solution (Figure
298 S5 in the Supplementary Information) modelled using the Hydra-Medusa software, which is
299 based on SOLGASWATER and HALTAFALL algorithms (Puigdomenech, 2013). Under
300 extremely acidic conditions (i.e., pH 1), In(III) removal efficiency was low at around 25%. This
301 could be explained by the high concentration of hydronium ions competing for binding sites on
302 the surface of the microalgal biomass. Once associated with the functional groups of the
303 biosorbent, hydronium ions restrict the adsorption of In^{3+} due to repulsive forces (Monteiro et
304 al, 2012). However, at higher pH values, several functional groups deprotonate and become
305 available for metal binding if the solution pH is greater than the functional group pK_a (Anslyn

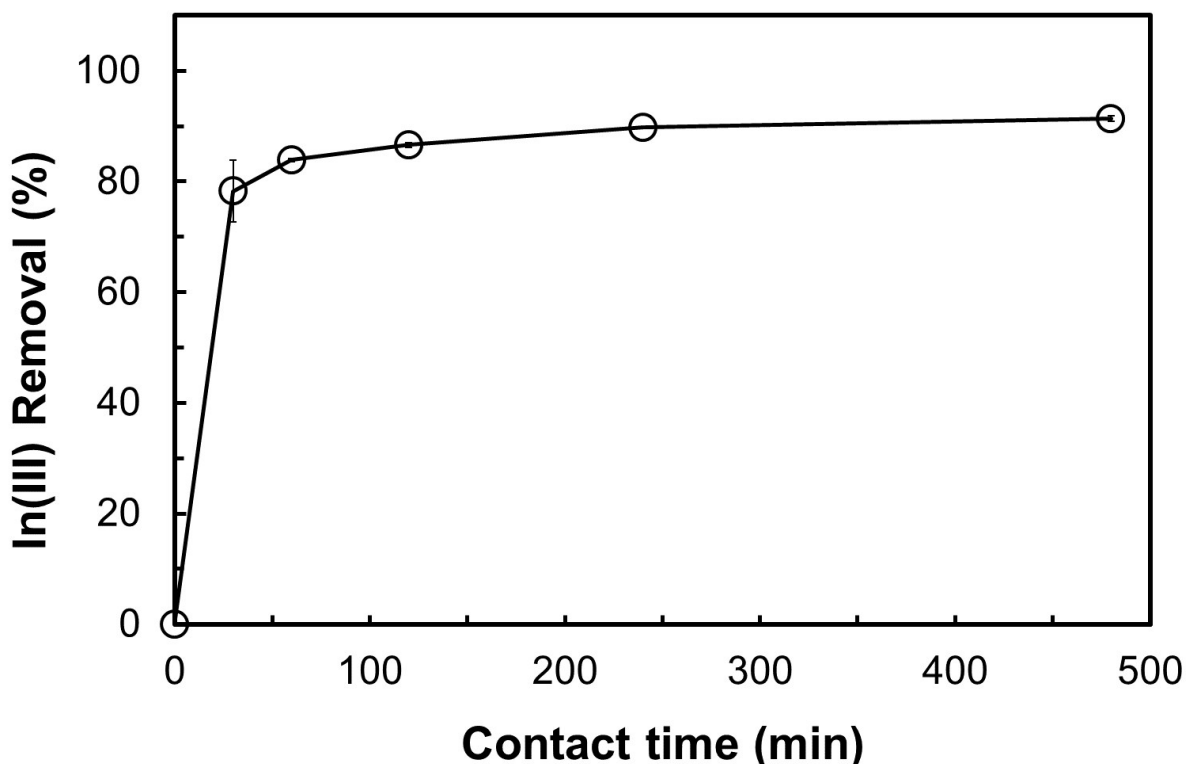
306 and Dougherty, 2006; Tran et al., 2017). For instance, the results of Boehm titration (Table 1)
307 suggested that carboxylic groups are present on the surface of the microalgal biomass. The pK_a
308 values of carboxylic acid groups range from 1.7 to 4.7 (Tran et al., 2017). At the upper range
309 of the tested pH values, carboxylic acid groups might have dissociated to form negatively
310 charged carboxylate groups, thus facilitating the higher In(III) adsorption at a final pH of 2.4.
311 The adsorbate-adsorbent system presented in this study was complex. Gadd (2009) commented
312 that the mechanisms involved in biosorption are often difficult to characterize, especially if the
313 biosorbent is biological in nature. Unlike chemically synthesized adsorbents, which have more
314 uniform composition and surface functional groups, different structural components are present
315 in most biosorbents. Many functional groups may be able to interact with the metal species to
316 varying degrees and may be influenced by physico-chemical factors. In general, different metal-
317 binding mechanisms are responsible for metal biosorption. In the case of indium biosorption by
318 microalgal biomass, multiple mechanisms may be involved, including electrostatic and
319 coordination interactions.

320 The results also indicate that microalgal biomass has an advantage when applied to real
321 wastewater or leach solutions since most of these have an acidic pH. This makes it more
322 competitive compared to most synthetic or chemically-modified adsorbents, which are either
323 unstable or inefficient when used in acidic conditions. For instance, multiwalled carbon
324 nanotubes (MWCNT) were reported to adsorb only 5% of the initial In(III) concentration (0.087
325 mM) at pH 4 (Alguacil et al., 2016). In another study by Calagui et al. (2014), chitosan-coated
326 bentonite beads were used to adsorb In(III). At an initial pH of 2, only 40% of the initial In(III)
327 concentration (0.17 mM) was removed by this adsorbent.

328 *3.5 Kinetics of indium biosorption*

329 Kinetics studies can give insights into the reaction pathways and mechanisms of the
330 adsorption reactions (Gupta et al., 2010). Indium biosorption kinetics were fast. The removal

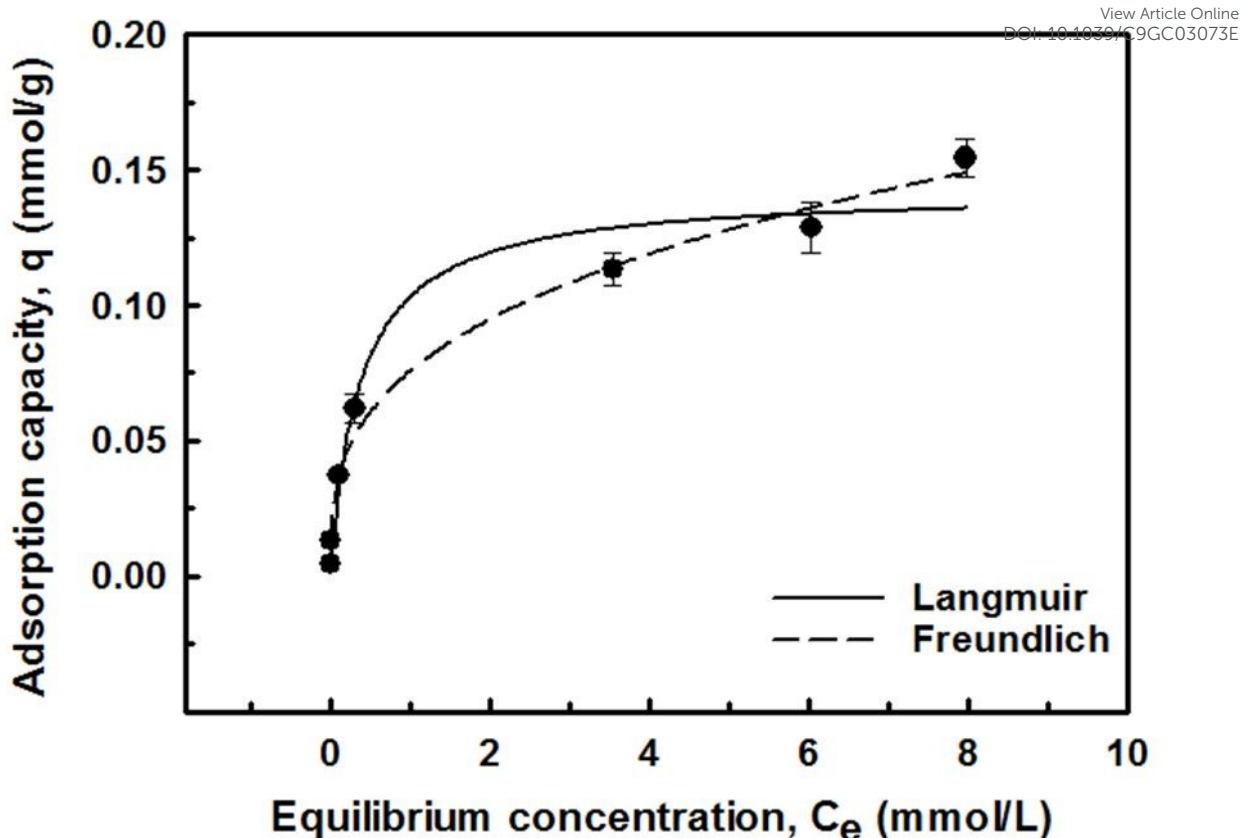
331 rapidly increased during the first minutes of the process, reaching up to ca. 80% of the initial
332 In(III) after 30 min (Figure 3). Fast kinetics are important for process scale-up. With rapid
333 adsorption, smaller reactor volumes are required, ensuring efficiency and economy (Aksu,
334 2002).



335
336 **Figure 3.** Kinetics of indium biosorption on microalgal biomass. Experimental conditions:
337 initial In(III) concentration = 0.15 mM; L/S ratio = 100 mL/g; initial pH 2; room temperature.

338 3.6 Biosorption isotherms

339 Indium biosorption was studied at different initial metal concentrations ranging from 0.05
340 to 10 mM. Langmuir and Freundlich isotherm models were fitted to the data (Figure 4). The
341 correlation coefficients suggest that the Freundlich model fits the data better than the Langmuir
342 model (Table 2). This can be an indication that In(III) was adsorbed in multilayers onto the
343 active sites of the microalgal biomass surface with lateral interaction between the adsorbed
344 molecules (Hwang et al., 2013).



345
346 **Figure 4.** Adsorption isotherms of indium onto microalgal biomass using the Langmuir and
347 Freundlich models. Experimental conditions: L/S ratio = 100 mL/g; initial pH 2; room
348 temperature.

349 **Table 2.** Constants and correlation coefficients of Langmuir and Freundlich models for indium
350 biosorption using microalgal biomass.

Isotherm model	Parameter	Value
<i>Langmuir</i>	q_{\max} (mmol/g)	0.14
	b (L/mmol)	2.64
	R^2	0.97
<i>Freundlich</i>	K_f (mmol $^{1-1/n}$ L $^{1/n}$ /g)	0.08
	n	3.07
	R^2	0.99

351
352 The maximum adsorption capacity (q_{\max}) of the microalgal biomass for In(III) at a final pH
353 of 2.4 was determined from the Langmuir model (Figure 4). The estimated q_{\max} value was 0.14

354 mmol/g, which is in the same order as those of adsorbents reported in the literature (Table 3).
355 However, because of different experimental conditions, the comparison among studies should
356 only be regarded as directional. Nevertheless, the microalgal biomass achieved a higher q_{\max}
357 compared to some chemically modified adsorbents, such as phosphorylated sawdust beads
358 (0.01 mmol/g) (Jeon et al., 2015). Furthermore, some adsorbents with higher q_{\max} values, such
359 as MWCNT and magnetite modified with amine polymer, were evaluated at pH values where
360 indium may precipitate as $\text{In}(\text{OH})_3$, overestimating the adsorption capacities of these adsorbents
361 (Alguacil et al., 2016; Chiou et al., 2015). Other synthetic adsorbents also showed better
362 adsorption capacity than the microalgal biomass. For instance, microbeads of poly(glycidyl
363 methacrylate-co-poly(ethylene glycol) diacrylate modified with iminodiacetic acid showed a
364 q_{\max} four times higher than that of the microalgal biomass (Hwang et al., 2013). However, the
365 production processes of synthetic adsorbents are often costly, complicated, and
366 environmentally unsustainable. These are crucial points to consider in the assessment of new
367 adsorbents, especially if the goal is to use the technology at industrial scale. The microalgal
368 biomass completely meets these conditions considering that no harmful and costly chemicals
369 are needed for its production. Moreover, microalgae can be grown on wastewater while
370 providing an economical and sustainable way of treating the wastewater through reduction of
371 BOD, N or P, and inhibition of coliforms (Abdel-Raouf et al., 2012). The use of the harvested
372 microalgal biomass as an effective $\text{In}(\text{III})$ biosorbent can add more value to the whole process
373 of resource recovery. Furthermore, only minimal handling is required before it can be used as
374 a biosorbent. In the current batch process, filtration using membrane syringe filters is a step that
375 accounts to a greater part of the total cost of the process. However, after process parameters
376 optimization through such batch experiments, biosorption could be performed as a continuous
377 flow process in columns with a filtration system that is not disposable and could be more cost-
378 effective in the long run.

379 **Table 3.** Maximum adsorption capacities of different adsorbents for indium ions.View Article Online
DOI: 10.1039/C9GC03073E

Adsorbent	Adsorbent modification	pH	q_{\max} (mmol/g)	Reference
Orange waste	Phosphorylation	2.0 ^a	0.71	Ghimire et al., 2008
Poly(vinylphosphonic acid-co-methacrylic acid) microbeads	-	8.0 ^c	0.71	Kwak et al., 2012
Poly(glycidyl methacrylate-co-poly(ethylene glycol) diacrylate) microbeads	Iminodiacetic acid	-	0.62	Hwang et al., 2013
Chitosan	Immobilization by bentonite, beads	4.0 ^a	0.16	Calagui et al., 2014
Sawdust	Phosphorylation, beads	3.5 ^b	0.01	Jeon et al., 2015
Magnetite	Amine polymer	4.5 ^b	0.48	Chiou et al., 2015
MWCNT	-	7.0 ^c	0.35	Alguacil et al., 2016
Microalgal biomass	-	2.4 ^b	0.14	This study

380 ^a Initial pH value. Authors did not report final equilibrium pH.381 ^b Final equilibrium pH382 ^c Authors did not report the potential contribution of In(OH)₃ precipitation to In(III) removal.383 *3.7 Effect of competing ions on indium biosorption*

384 The interference of other ions present in the matrix is another key parameter in evaluating
 385 the performance of microalgal biomass for indium biosorption. For instance, ITO etching
 386 wastewater—a secondary source of In(III)—contains Al(III), Cu(II), and Sn(II) (Swain et al.,
 387 2015). The presence of these ions might affect the performance of adsorbents for indium
 388 adsorption due to the competition for binding sites. However, most indium adsorption studies
 389 reported in the literature only focused on single metal solutions. The possible competition for
 390 adsorption sites was not evaluated, presenting a disadvantage considering that the goal of these

391 studies is to use the adsorbents in real and complex waste streams. In the present work, the
392 competing effects of Cu(II), Zn(II), Sn(II), Al(III), and Fe(III) on indium biosorption were
393 examined (Figure 5). Despite the concentrations of these competing ions being 10 times higher
394 than that of In(III), selectivity of In(III) was observed over Cu(II), Zn(II), and Al(III). This is
395 remarkable considering that the biosorbent was not treated or modified. For instance, Zn(II)
396 was not adsorbed on the microalgal biomass, favoring In(III) adsorption at ca. 55% of the initial
397 In(III) concentration. In a study by Kwon and Jeon (2012a), selective adsorption of In(III) over
398 Zn(II) was also observed using phosphorylated sawdust. However, the adsorption experiments
399 were conducted at pH 3.5 and the potential contribution of In(OH)₃ precipitation to In(III)
400 removal was not reported. Nevertheless, this study by Kwon and Jeon (2012a) explained the
401 possible reason for selective In(III) adsorption through the Hard and Soft Acids and Bases
402 (HSAB) theory. The phosphate groups of the phosphorylated sawdust are classified as hard
403 base. These strongly bind with In(III), which is a hard acid, as opposed to Zn(II), which is an
404 intermediate (borderline) acid. This could be one of the reasons for the selective In(III) removal
405 by the microalgal biomass considering that microalgae cell walls were reported to have
406 phosphate groups (Suresh Kumar et al., 2015), which was also indicated by the FTIR results
407 (Figure 1). However, for future study, nuclear magnetic resonance (NMR) could be performed
408 to further investigate the interaction between the indium ions and the phosphate groups. This
409 could complement the results obtained from FTIR spectroscopy by verifying the active sites of
410 the microalgal biomass.

411

412

413

414

415

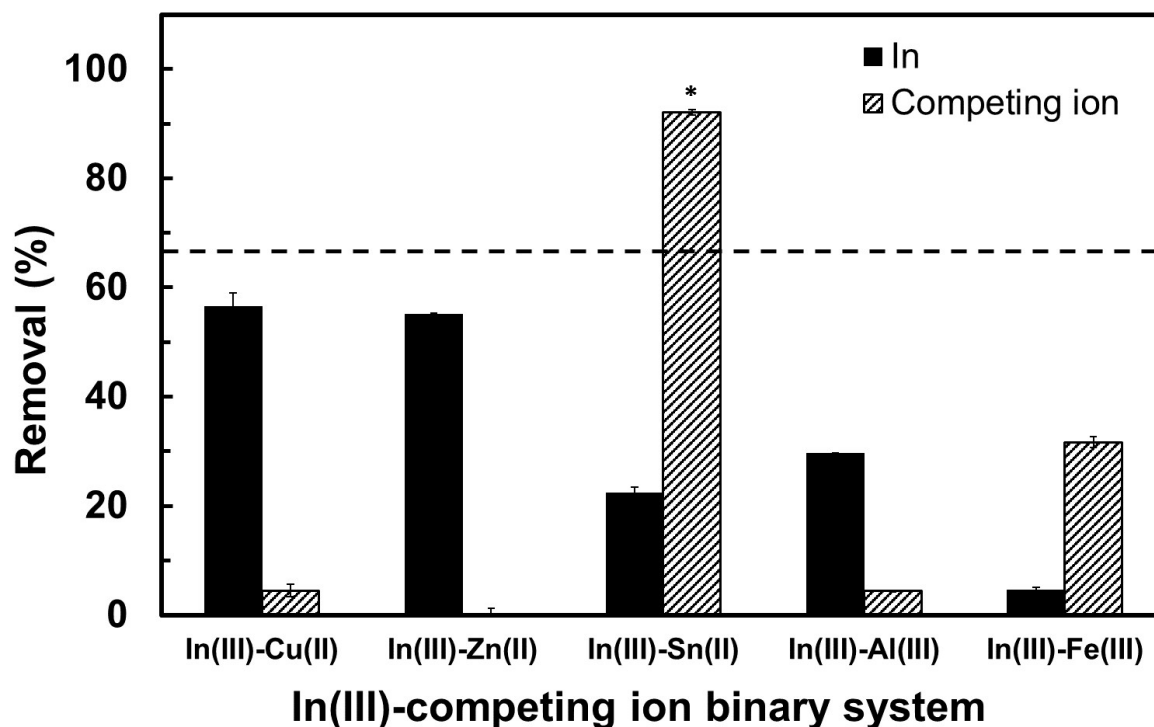


Figure 5. Effect of competing ions on the adsorption of In(III) using microalgal biomass. The dashed line represents the removal efficiency of the microalgal biomass for In(III) without competing ions present in the system. Experimental conditions: initial In(III) concentration = 1 mM; initial concentration of competing ion = 10 mM; L/S ratio = 100 mL/g; initial pH 2; room temperature. * The results of the control experiments showed that Sn(II) removal was mostly because of precipitation.

The results suggest that microalgal biomass can be an effective biosorbent, even in solutions where Cu(II), Zn(II), and Al(III) are present. However, although selectivity was observed, the removal efficiency of microalgal biomass for In(III) decreased to some extent because of the high concentrations of competing ions (Figure 5). The presence of Cu(II) in the solution affected In(III) biosorption the least as the removal efficiency for In(III) decreased only by about 10 %. In order to attain complete removal of In(III) in the presence of Cu(II), the amount of the microalgal biomass can be increased since it is an inexpensive and sustainable material.

441 For instance, assuming that the adsorption capacity would remain almost constant, a L/S ratio
442 of 50 mL/g or lower could potentially achieve complete In(III) adsorption in a system with 1
443 mM In(III) and 10 mM Cu(II). On the other hand, In(III) removal efficiency drastically
444 decreased from 67 % to 5 % when Fe(III) was present in the system. A relatively high Fe(III)
445 removal efficiency was observed for the microalgal biomass (ca. 32 % of the initial Fe(III)
446 concentration), which indicates that Fe(III) and In(III) most likely compete for the same
447 adsorption sites. Co-adsorption of Fe is a problem in Fe-rich solutions. This lack of selectivity
448 between In(III) and Fe(III) was also observed by Van Roosendael et al. (2019) in their study of
449 adsorption of In(III) from aqueous solutions using an Aliquat 336 (chloride) supported ionic
450 liquid phase (SILP). Because of co-adsorption of In(III) and Fe(III), the initial Aliquat 336
451 (chloride) SILP was replaced with an Aliquat 336 (iodide) SILP on the basis that indium forms
452 complexes with iodide species, while iron does not. An excess of iodide ions was added to the
453 aqueous solution to form indium iodide species, which are adsorbed to the Aliquat 336 (iodide)
454 SILP. Furthermore, Fe powder was added to the solution to reduce Fe(III) to Fe(II), thereby
455 improving In(III) selectivity. This approach emphasizes the need to understand the surface
456 chemistry of the adsorbent and nature of molecular interactions in order to attain In(III)
457 selectivity over Fe(III). However, this also highlights that even costly and synthetic adsorbents
458 encounter problems in Fe-rich solutions. Thus, the balance between the adsorbent performance
459 and its cost-effectiveness should be evaluated.

460 In the case of the In-Sn system, about 92 % of the initial Sn(II) concentration was removed
461 from the solution, which would correspond to an adsorption capacity of 0.76 mmol/g. However,
462 the Sn(II) removal can be largely attributed to precipitation as it was observed that white
463 insoluble solids were formed during the incubation. Furthermore, light scattering measurements
464 detected the formation of amorphous Sn(OH)₂ particles in SnCl₂ solutions at pH values between

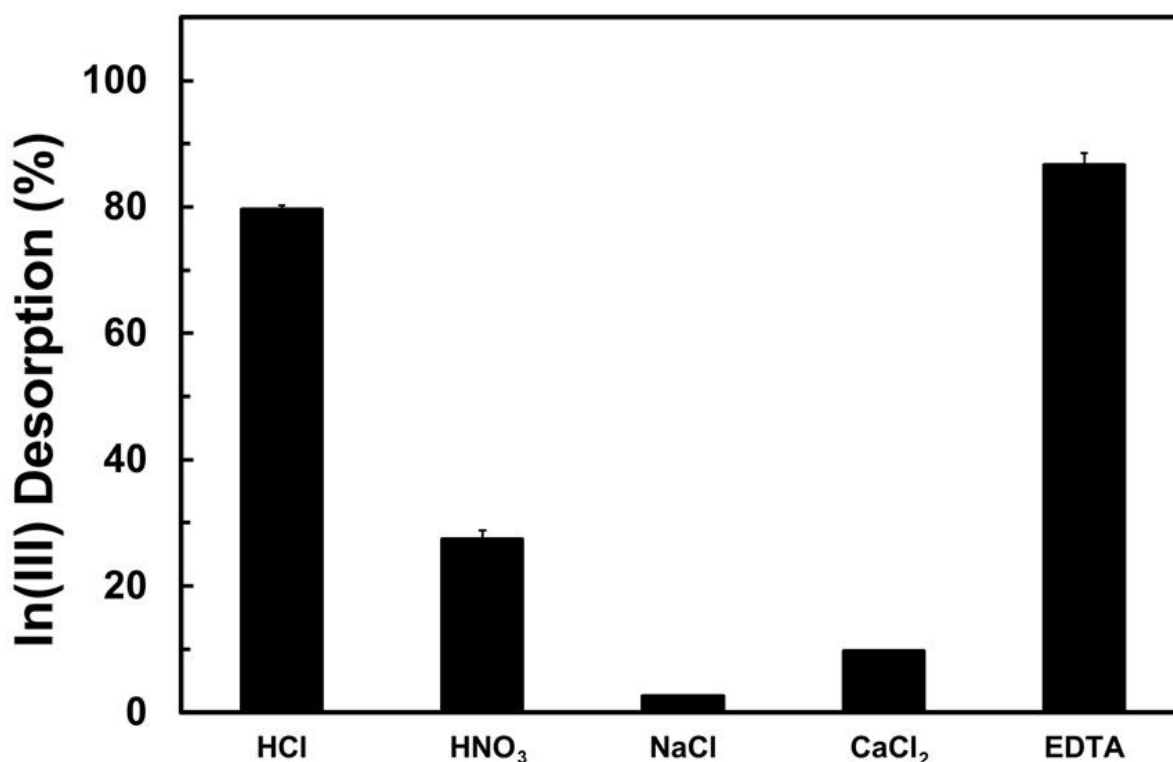
465 2.0 and 2.5 (Cigala et al., 2012). This supports the observation of tin precipitation because the
466 final pH of the solution was around pH 2.

467 3.8 Microalgal biomass regeneration

468 Adsorbent regeneration is an essential aspect of the adsorption process as it could contribute
469 to the overall cost-effectiveness of the technology (Lata et al., 2015). For effective regeneration,
470 the desorption process must restore the adsorbent close to its initial properties, especially the
471 preservation of its adsorption capacity, to allow its reuse in multiple adsorption-desorption
472 cycles. However, the desorption of metal-laden adsorbents is a complex process that involves
473 several factors, such as the type of the desorbing agent, desorption time, temperature, solution
474 pH, and the adsorbent surface properties (Lata et al., 2015). In general, metal desorption from
475 biosorbents involves lowering the pH of the solution as this will cause the displacement of metal
476 cations back to the solution (Monteiro et al., 2012). The most commonly used desorbing agents
477 are inorganic acids, followed by inorganic salts, chelating agents, and organic acids (Suresh
478 Kumar et al., 2015).

479 As an initial step to assess the regenerability of microalgal biomass, the desorption of In(III)
480 was investigated using 0.1 M HCl, HNO₃, NaCl, CaCl₂, and EDTA. The highest In(III)
481 desorption efficiency was obtained with EDTA with 87 % In(III) desorbed, followed by HCl
482 with 80 % (Figure 6). Considering both the efficiency and economic feasibility, HCl was chosen
483 as desorbing agent for the succeeding regeneration experiments. Desorption studies of
484 previously adsorbed In(III) on phosphorylated sawdust were also investigated by Kwon and
485 Jeon (2012b). Although the desorption efficiency of HCl was lower than those of nitrilotriacetic
486 acid (NTA) and EDTA, HCl was also chosen as the best desorbing agent for indium ions
487 considering the cost-effectiveness, although a relatively high HCl concentration of 0.5 M was
488 used in this study. The desorption process using HCl as the desorbing agent occurs chemically
489 through the exchange of In(III) for protons. When HCl is added to the In-loaded biomass, the

490 biosorbent surface is completely covered with H^+ ions, while the coordination spheres of
491 adsorbed indium ions are disrupted. In this way, the indium ions cannot compete with H^+ ions
492 for adsorption sites, causing the indium ions to be released from the biosorbent surface into the
493 solution (Bansal et al., 2009). The generated effluents from the desorption process are acidic in
494 nature.
495

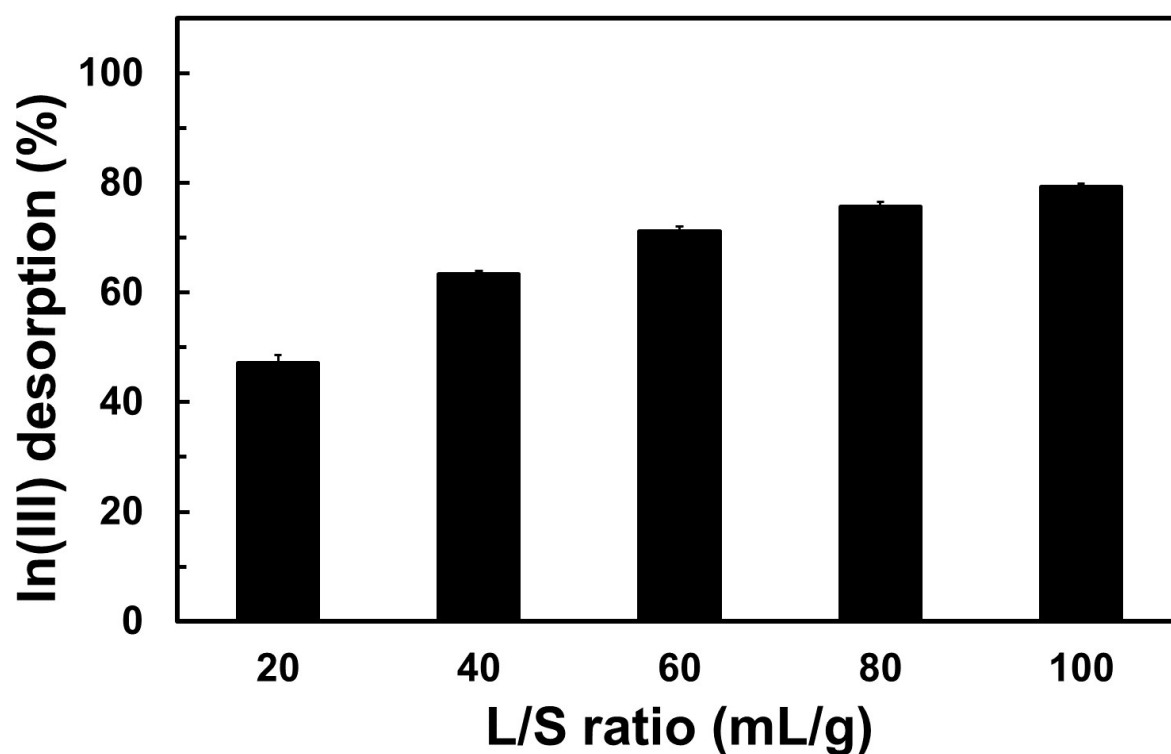


496
497 **Figure 6.** Indium desorption efficiencies of various desorbing agents. Experimental conditions:
498 loaded amount of indium onto microalgal biomass = 1.50 mg/g; concentration of desorbing
499 agent = 0.1 M; L/S ratio = 100 mL/g; contact time = 24 hours; room temperature.

500 The process of upconcentrating the indium ions was investigated by desorbing the In-loaded
501 microalgal biomass with different volumes of 0.1 M HCl. Several L/S ratios ranging from 20
502 to 100 mL/g were tested. As the L/S ratio increased, the desorption efficiency increased as well
503 (Figure 7). The highest desorption efficiency (ca. 80 %) was obtained using a L/S ratio of 100

504 mL/g. Considering different factors, such as upconcentration, cost-effectiveness, and
505 efficiency, a L/S ratio of 60 mL/g was used for the succeeding desorption experiments. This
506 has a desorption efficiency of 72% after 24 hours. Subsequently, the desorption kinetics using
507 this L/S ratio was investigated. The desorption of the In(III) fraction loosely bonded to the
508 microalgal biomass occurred very fast (Figure 8). After 30 minutes, a desorption efficiency of
509 about 70% was obtained, which is similar to that obtained after 24 hours. Thus, a 30-minute
510 contact time was used for the next adsorption-desorption experiments.

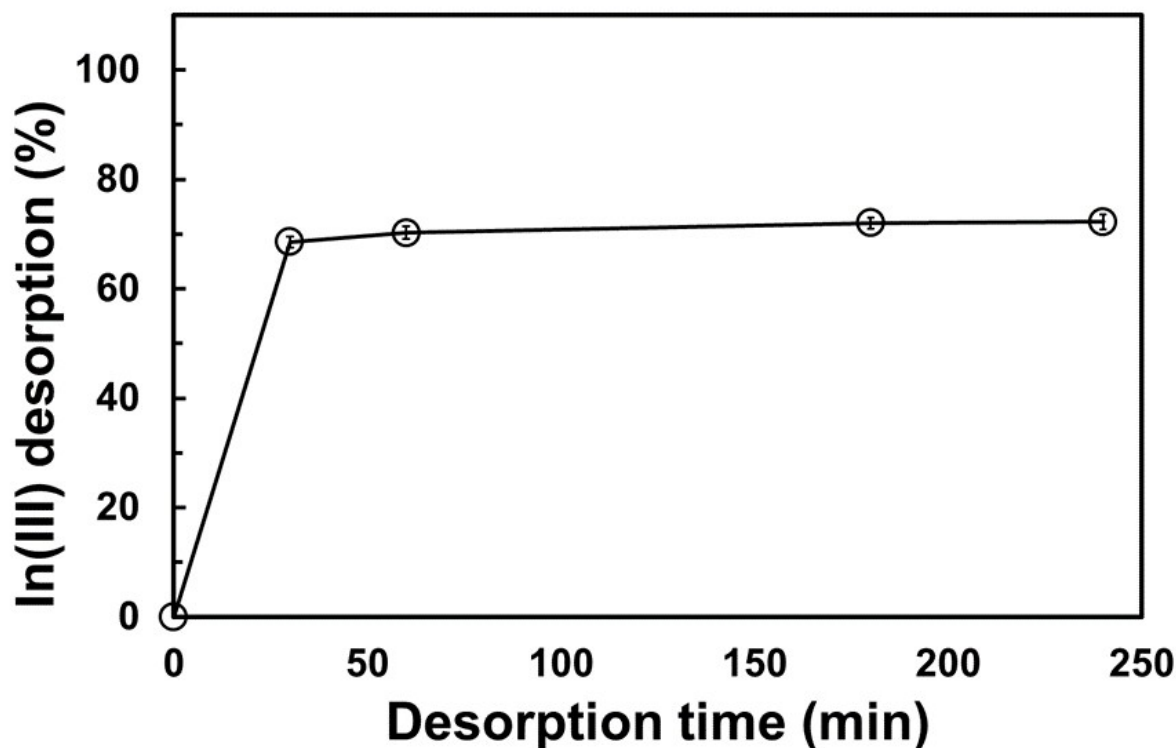
511



512

513 **Figure 7.** Effect of the liquid/solid (L/S) ratio on the desorption efficiency of indium ions using
514 0.1 M HCl. Experimental conditions: loaded amount of indium onto microalgal biomass = 1.50
515 mg/g; contact time = 24 hours; room temperature.

516

View Article Online
DOI: 10.1039/C9GC03073E

517

518 **Figure 8.** Change of desorption efficiency of indium ions with time using 0.1 M HCl.
519 Experimental conditions: loaded amount of indium onto microalgal biomass = 1.50 mg/g; L/S
520 ratio = 60 mL/g; room temperature.

521 3.9 Microalgal biomass reusability

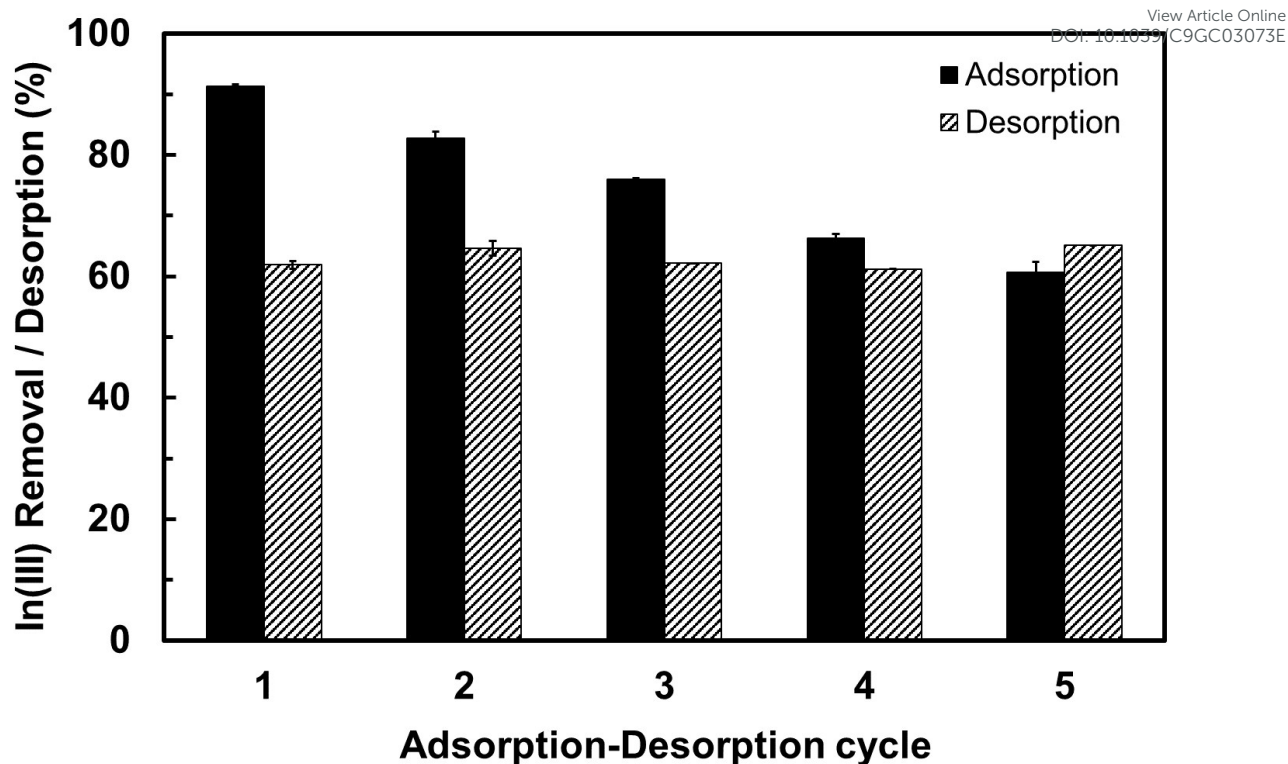
522 Stability of the adsorbent should be investigated if it will be reused in multiple adsorption
523 and desorption cycles. Figure 9 shows five cycles of In(III) adsorption-desorption performed
524 using 0.1 M HCl as desorbing agent. In general, the adsorption capacity of the microalgal
525 biomass for In(III) progressively decreased with increasing number of adsorption-desorption
526 cycles. After five cycles, the In(III) removal decreased from 91.3% to 60.7%. Similarly,
527 cadmium adsorption on the microalga *Spirulina platensis* immobilized in alginate and silica gel
528 decreased by about 30% after five regeneration cycles using 0.1 M HCl as desorbing agent
529 (Rangsayatorn et al., 2004). The decrease in the microalgal biomass adsorption capacity can
530 possibly be due to two reasons. First, the fraction of indium ions remaining on the biosorbent

531 surface after every regeneration cycle result in a decrease in the number of available adsorption
532 sites. Second, the active functional groups on the microalgal biomass surface are partially
533 destroyed by the desorbing agent after each desorption step. Figure S6 shows a SEM image of
534 the microalgal biomass after In(III) desorption using 0.1 M HCl. Although the changes in the
535 surface texture of the biosorbent are still not apparent, it can be observed that some parts were
536 damaged. However, even synthetic adsorbents can exhibit decreased adsorption capacities after
537 several adsorption-desorption cycles. For instance, Chiou et al. (2015) determined the
538 reusability of amide group-functionalized magnetite in In(III) adsorption by using 0.01 M
539 HNO₃ as a desorbing agent. During the third adsorption-desorption cycle, the adsorption
540 capacity of the adsorbent exhibited a loss of about 53%, which was reported to be possibly
541 caused by the detachment of the ethylenediamine from the magnetite surface during the
542 recycling processes. This suggests that the stability of the adsorbents should also be part of the
543 assessment of the adsorbent. Furthermore, another factor to consider when assessing
544 adsorption-desorption cycles is the metal upconcentration. In this study, a concentration ratio
545 (i.e., ratio of In(III) concentration in the desorbed solution to In(III) concentration in the initial
546 solution) of about 1.5 was achieved after the adsorption and desorption steps. Since this value
547 is limited, other ways to recover In(III) can be explored, especially that it exhibited a high In(III)
548 selectivity. One option could be burning the indium-loaded microalgae to end up with an
549 indium-rich ash, which could be subsequently processed in a metal-processing plant.

550

551

552



553

554 **Figure 9.** Five cycles of In(III) adsorption – desorption using 0.1 M HCl as desorbing agent.

555 Experimental conditions: Adsorption – $C_0 = 0.15$ mM; L/S ratio = 100 mL/g; contact time = 24

556 hours; room temperature; Desorption – L/S ratio = 60 mL/g; contact time = 30 minutes; room

557 temperature.

558 4. Conclusions

559 This study investigated the effects of various process parameters—specifically pH, contact

560 time, initial metal concentration, presence of competing ions, and desorption—on the

561 biosorption of In(III) onto microalgal biomass. Results showed that this biosorbent has a

562 maximum In(III) adsorption capacity of 0.14 mmol/g at an initial pH value of 2. Further analysis

563 revealed that the adsorption equilibrium data were well-fitted by the Freundlich isotherm

564 model, suggesting that indium ions were adsorbed in multilayers onto the active sites of the

565 microalgal biomass surface. The kinetics data showed that In(III) biosorption by microalgal

566 biomass is a fast process, attaining 80% In(III) removal within a contact time of 30 minutes. In

567 addition, selectivity of In(III) was observed over Cu(II), Zn(II), and Al(III) despite the high

568 concentrations of these metals. Moreover, In(III) ions adsorbed on microalgal biomass could
569 be effectively desorbed by 0.1 M HCl, but burning the In-loaded biosorbent to obtain an In-rich
570 ash is also an option to recover In(III). Overall, this study demonstrated the potential of
571 microalgal biomass for In(III) biosorption from aqueous solutions. This potential should now
572 be further explored using real indium-containing wastewaters and leachates. Furthermore, it
573 provided some insight into the adsorption behavior and mechanism of In(III) adsorption on
574 microalgal biomass. This information can now be used as input data for subsequent continuous
575 adsorption experiments in a column setup.

576 **5. Conflict of interest**

577 The authors declare no conflict of interest.

578 **6. Acknowledgements**

579 This study was partly supported by METGROW+, a project of the European Union's
580 Horizon 2020 research and innovation programme under grant agreement No 690088. N. R. N.
581 acknowledges the UGent Special Research Fund (BOF) for the PhD scholarship. L. O. G.
582 acknowledges METGROW+ for the post-doctoral scholarship. L. A. acknowledges the
583 European Union's Horizon 2020 research and innovation programme under the Marie
584 Skłodowska-Curie grant agreement No 676070 (MSCA-ITN project SuPER-W) for her PhD
585 scholarship. M. G. acknowledges the Spanish Ministry of Economy and Competitiveness
586 (RYC-2016-20059).

587 **7. References**

588 Abdel-Raouf, N., Al-Homaidan, A. A., & Ibraheem, I. B. M. (2012). Microalgae and
589 wastewater treatment. *Saudi Journal of Biological Sciences*, 19(3), 257-275.

590 Aksu, Z. (2002). Determination of the equilibrium, kinetic and thermodynamic parameters of
591 the batch biosorption of nickel(II) ions onto *Chlorella vulgaris*. *Process Biochemistry*, 38(1),
592 89-99.

- 593 Alfantazi, A. M., & Moskalyk, R. R. (2003). Processing of indium: a review. *Minerals*
594 *Engineering*, 16(8), 687-694. View Article Online
DOI: 10.1039/C9GC03073E
- 595 Alguacil, F. J., Lopez, F. A., Rodriguez, O., Martinez-Ramirez, S., & Garcia-Diaz, I. (2016).
596 Sorption of indium (III) onto carbon nanotubes. *Ecotoxicology and Environmental Safety*, 130,
597 81-86.
- 598 Anslyn, E. V., & Dougherty, D. A. (2006). *Modern physical organic chemistry*. Sausalito, CA
599 University Science Books.
- 600 Arashiro, L., Ferrer, I., Rousseau, D.P.L., Van Hulle, S.W.H., & Garfí, M. (2019). The effect
601 of primary treatment of wastewater in high rate algal pond systems: Biomass and bioenergy
602 recovery. *Bioresource Technology*, 280.
- 603 Bakatula, E. N., Richard, D., Neculita, C. M., & Zagury, G. J. (2018). Determination of point
604 of zero charge of natural organic materials. *Environmental Science and Pollution Research*.
- 605 Bandosz, T., Biggs, M., Gubbins, K. E., Hattori, Y., Liyama, T., Kaneko, K., Pikunic, J. P.,
606 and Thomson, K. T. (2003). Molecular models of porous carbons. *Chemistry and Physics of*
607 *Carbon*, 28, 41-218.
- 608 Bansal, M., Singh, D., Garg, V. K., & Rose, P. (2009). Use of agricultural waste for the removal
609 of nickel ions from aqueous solutions: Equilibrium and kinetics studies. *International Journal*
610 *of Civil and Environmental Engineering*, (3), 174-180.
- 611 Boehm, H. P. (2002). Surface oxides on carbon and their analysis: a critical assessment. *Carbon*,
612 40(2), 145-149.
- 613 Calagui, M. J. C., Senoro, D. B., Kan, C.-C., Salvacion, J. W. L., Futralan, C. M., & Wan, M.-
614 W. (2014). Adsorption of indium(III) ions from aqueous solution using chitosan-coated
615 bentonite beads. *Journal of Hazardous Materials*, 277, 120-126.

- 616 Chiou, C.-S., Chuang, K.-J., Chen, H.-W., & Chen, Y.-C. (2015). Magnetite modified with
617 amine polymer to adsorb indium ions. *Powder Technology*, 279, 247-253. View Article Online
DOI: 10.1039/C9GC03073E
- 618 Chou, W.-S., Shen, Y.-H., Yang, S.-J., Hsiao, T.-C., & Huang, L.-F. (2016). Recovery of
619 indium from the etching solution of indium tin oxide by solvent extraction. *Environmental
620 Progress & Sustainable Energy*, 35(3), 758-763.
- 621 Cigala, R. M., Crea, F., De Stefano, C., Lando, G., Milea, D., & Sammartano, S. (2012). The
622 inorganic speciation of tin(II) in aqueous solution. *Geochimica et Cosmochimica Acta*, 87, 1-
623 20.
- 624 Dmytryk, A., Saeid, A., & Chojnacka, K. (2014). Biosorption of Microelements by Spirulina:
625 Towards Technology of Mineral Feed Supplements. *The Scientific World Journal*, 2014, 15.
- 626 European Commission (2017, September 13). Communication from the Commission to the
627 European Parliament, the Council, the European Economic and Social Committee and the
628 Committee of the Regions on the 2017 list of Critical Raw Materials for the EU. Retrieved from
629 [http://eur-lex.europa.eu/legal-content/EN/TXT/HTML/?uri=CELEX:52017DC0490&from=](http://eur-lex.europa.eu/legal-content/EN/TXT/HTML/?uri=CELEX:52017DC0490&from=EN)
630 EN.
- 631 Faria, P. C. C., Órfão, J. J. M., & Pereira, M. F. R. (2004). Adsorption of anionic and cationic
632 dyes on activated carbons with different surface chemistries. *Water Research*, 38(8), 2043-
633 2052.
- 634 Felix, N. (2000). Indium and Indium Compounds. In *Ullmann's Encyclopedia of Industrial
635 Chemistry*, (Ed.).
- 636 Fortes, M. C. B., Martins, A. H., & Benedetto, J. S. (2003). Indium adsorption onto ion
637 exchange polymeric resins. *Minerals Engineering*, 16(7), 659-663.

- 638 Gadd, G. M. (2009). Biosorption: critical review of scientific rationale, environmental
639 importance and significance for pollution treatment. *Journal of Chemical Technology &*
640 *Biotechnology*, 84(1), 13-28.
- 641 Ghimire, K. N., Inoue, J. i., Inoue, K., Kawakita, H., & Ohto, K. (2008). Adsorptive Separation
642 of Metal Ions onto Phosphorylated Orange Waste. *Separation Science and Technology*, 43(2),
643 362-375.
- 644 Gupta, V. K., Rastogi, A., & Nayak, A. (2010). Biosorption of nickel onto treated alga
645 (*Oedogonium hatei*): Application of isotherm and kinetic models. *Journal of Colloid and*
646 *Interface Science*, 342(2), 533-539.
- 647 Hasegawa, H., M M Rahman, I., Umehara, Y., Sawai, H., Maki, T., Furusho, Y., & Mizutani,
648 S. (2013). Selective Recovery of Indium from the Etching Waste Solution of the Flat-panel
649 Display Fabrication Process. *Microchemical Journal*, 110, 133-139.
- 650 Hwang, C. W., Kwak, N. S., & Hwang, T. S. (2013). Preparation of poly(GMA-co-PEGDA)
651 microbeads modified with iminodiacetic acid and their indium adsorption properties. *Chemical*
652 *Engineering Journal*, 226, 79-86.
- 653 Jeon, C., Cha, J.-H., & Choi, J.-Y. (2015). Adsorption and recovery characteristics of
654 phosphorylated sawdust bead for indium(III) in industrial wastewater. *Journal of Industrial and*
655 *Engineering Chemistry*, 27, 201-206.
- 656 Koleini, S. M. J., Mehrpouya, H., Saberyan, K., & Abdolahi, M. (2010). Extraction of indium
657 from zinc plant residues. *Minerals Engineering*, 23(1), 51-53.
- 658 Kwak, N.-S., Baek, Y., & Hwang, T. S. (2012). The synthesis of poly(vinylphosphonic acid-
659 co-methacrylic acid) microbeads by suspension polymerization and the characterization of their
660 indium adsorption properties. *Journal of Hazardous Materials*, 203-204, 213-220.

- 661 Kwon, T.-N., & Jeon, C. (2012a). Selective adsorption for indium(III) from industrial wastewater using chemically modified sawdust. Korean Journal of Chemical Engineering, 29(12), 1730-1734. View Article Online
DOI: 10.1039/C9GC03073E
- 662
663
- 664 Kwon, T.-N., & Jeon, C. (2012b). Desorption and Regeneration Characteristics for Previously Adsorbed Indium Ions to Phosphorylated Sawdust. Environmental Engineering Research, 17(2), 65-67.
- 665
666
- 667 Lata, S., Singh, P. K., & Samadder, S. R. (2015). Regeneration of adsorbents and recovery of heavy metals: a review. International Journal of Environmental Science and Technology, 12(4), 1461-1478.
- 668
669
- 670 Maurya, R., Ghosh, T., Paliwal, C., Shrivastav, A., Chokshi, K., Pancha, I., . . . Mishra, S. (2014). Biosorption of Methylene Blue by De-Oiled Algal Biomass: Equilibrium, Kinetics and Artificial Neural Network Modelling. PLOS ONE, 9(10), e109545.
- 671
672
- 673 Monteiro, C. M., Castro, P. M. L., & Malcata, F. X. (2012). Metal uptake by microalgae: Underlying mechanisms and practical applications. Biotechnology Progress, 28(2), 299-311.
- 674
675
- 676 Ogi, T., Tamaoki, K., Saitoh, N., Higashi, A., & Konishi, Y. (2012). Recovery of indium from aqueous solutions by the Gram-negative bacterium *Shewanella* algae. Biochemical Engineering Journal, 63, 129-133.
- 677
678
- 679 Orko, I., Kangas, P., Lundström, M., & Koukkari, P. (2016). Hydrometallurgical Processing of Jarosite Waste to Value-Added Products. Bergamo, Italy, 3rd Symposium on Urban Mining and Circular Economy SUM 2016.
- 680
681
- 682 Puigdomenech, I. (2013, April 26). Medusa: Chemical Equilibrium Diagrams. Retrieved from <https://www.kth.se/che/medusa/chemeq-1.369367>

- 683 Rangsayatorn, N., Pokethitiyook, P., Upatham, E. S., & Lanza, G. R. (2004). Cadmium
684 biosorption by cells of *Spirulina platensis* TISTR 8217 immobilized in alginate and silica gel.
685 *Environment International*, 30(1), 57-63.
- 686 Rocchetti, L., Amato, A., Fonti, V., Ubaldini, S., De Michelis, I., Kopacek, B., Veglio, F., &
687 Beolchini, F. (2015). Cross-current leaching of indium from end-of-life LCD panels. *Waste*
688 *Management*, 42, 180-187.
- 689 Schwarz-Schampera, U. (2014). *Indium Critical Metals Handbook* (pp. 204-229): John Wiley
690 & Sons.
- 691 Schwarz-Schampera, U., & Herzig, P. M. (2002). *Introduction Indium: Geology, Mineralogy,*
692 *and Economics* (pp. 1-7). Berlin, Heidelberg: Springer Berlin Heidelberg.
- 693 Sun, Z., Cao, H., Xiao, Y., Sietsma, J., Jin, W., Agterhuis, H., & Yang, Y. (2017). Toward
694 Sustainability for Recovery of Critical Metals from Electronic Waste: The Hydrochemistry
695 Processes. *ACS Sustainable Chemistry & Engineering*, 5(1), 21-40.
- 696 Suresh Kumar, K., Dahms, H.-U., Won, E.-J., Lee, J.-S., & Shin, K.-H. (2015). Microalgae –
697 A promising tool for heavy metal remediation. *Ecotoxicology and Environmental Safety*, 113,
698 329-352.
- 699 Swain, B., Mishra, C., Hong, H. S., Cho, S.-S., & Lee, S. k. (2015). Commercial process for
700 the recovery of metals from ITO etching industry wastewater by liquid–liquid extraction:
701 simulation, analysis of mechanism, and mathematical model to predict optimum operational
702 conditions. *Green Chemistry*, 17(7), 3979-3991.
- 703 Tarkan, H. M., & Finch, J. A. (2005). Air-assisted solvent extraction: towards a novel extraction
704 process. *Minerals Engineering*, 18(1), 83-88.

- 705 Tran, H. N., You, S.-J., Hosseini-Bandegharai, A., & Chao, H.-P. (2017). Mistakes and
706 inconsistencies regarding adsorption of contaminants from aqueous solutions: A critical review.
707 Water Research, 120, 88-116.
- 708 United States Geological Survey (USGS). (2017, January). Mineral Commodity Summaries:
709 Indium. Retrieved from [https://minerals.usgs.gov/minerals/pubs/commodity/indium/mcs-](https://minerals.usgs.gov/minerals/pubs/commodity/indium/mcs-2017-indiu.pdf)
710 [2017-indiu.pdf](https://minerals.usgs.gov/minerals/pubs/commodity/indium/mcs-2017-indiu.pdf)
- 711 Van Roosendael, S., Regadío, M., Roosen, J., & Binnemans, K. (2019). Selective recovery of
712 indium from iron-rich solutions using an Aliquat 336 iodide supported ionic liquid phase
713 (SILP). Separation and Purification Technology, 212, 843-853.
- 714 Wegscheider, S., Steinlechner, S., & Leuchtenmüller, M. (2017). Innovative Concept for the
715 Recovery of Silver and Indium by a Combined Treatment of Jarosite and Electric Arc Furnace
716 Dust. JOM, 69(2), 388-394.
- 717 Wilde, E. W., & Benemann, J. R. (1993). Bioremoval of heavy metals by the use of microalgae.
718 Biotechnology Advances, 11(4), 781-812.
- 719 Wilson, B. P., Halli, P., Orko, I., Kangas, P., Lundström, M., & Koukkari, P. (2016). Value-
720 added materials from the hydrometallurgical processing of jarosite waste. E3S Web Conf., 8,
721 01015.
- 722 Yang, J., Retegan, T., & Ekberg, C. (2013). Indium recovery from discarded LCD panel glass
723 by solvent extraction. Hydrometallurgy, 137, 68-77.
- 724 Zhang, F., Wei, C., Deng, Z., Li, X., Li, C., & Li, M. (2016). Reductive leaching of indium-
725 bearing zinc residue in sulfuric acid using sphalerite concentrate as reductant. Hydrometallurgy,
726 161, 102-106.